Investigation of systematic errors for analysis with DC and ScFi

V.V.Yazkov (SINP, Moscow)

March 11, 2008

Abstract

Main sources of systematic errors are investigated for mode of analysis which uses coordinate information from DC and ScFi. Estimation of systematic error values are presented.

Introduction

The inaccuracy of background event description ("Coulomb" pairs mainly) and also simulated distributions of "atomic" pairs leads to occurrence of systematic errors at calculation of atom breakup probability P_{br} and therefore systematic errors of $A_{2\pi}$ lifetime measurement.

Main sources of systematic errors are:

1. An admixture of non-identified K^+K^- and $p\overline{p}$ pairs.
2. Finite size of production region. Cross section of atom production is calculated in approximation of point-like sources of pions. However there are correction due to finite size of production region and strong interaction in the final state [1].
3. The error in an estimation of multiple scattering for detectors and elements of the DIRAC setup.
4. Finite double-track resolution of fiber detector.
5. Presence of hits from background particles in ScFi and IH.
6. Accuracy of trigger system simulation.
7. Correction on a width of reconstructed Λ hyperon which is used for calibration of the setup resolution. The error of laboratory momentum reconstruction is increased by 10% for simulated events. It provides the same width of reconstructed Λ-peak for experimental and simulated data.

1 Admixture of non-identified K^+K^- and $p\overline{p}$ pairs

Threshold Cherenkov counters and muon detectors of setup DIRAC [2] allow to exclude an admixture of the pairs, consisting of electrons, positrons, or muons. All hadron pairs are considered to be $\pi^+\pi^-$. The most dangerous admixture is an admixture of pairs which consist of two oppositely charged particles of equal mass. At the condition of the DIRAC experiment this is mainly K^+K^- for whole momentum range, and $p\overline{p}$ pairs with lab momentum of particles more than 1.8 GeV/c. Protons (antiprotons) with $P_{Lab} < 1.8$ GeV/c are rejected by cut on the difference of times measured by VH and upstream detectors.

Non-identified K^+K^- and $p\overline{p}$ are analyzed in assumption that they are pions. From Lorentz transformation it is known that in this case transverse components of relative momentum in pair CMS Q_X, Q_Y are measured correctly but longitudinal component Q_L is underestimated by factor $\approx m_\pi/m_K$ (m_π/m_p). As result these pairs also form peak due to Coulomb interactions in a final state for particles with small relative momentum Q but width of this peak other, than for $\pi^+\pi^-$. It leads to error in description of "Coulomb" pair background which following to an error in number of "atomic" pairs and breakup probability value.

Estimation of $p\overline{p}$ was done in [3], using time-of-flight measurement by upstream detectors (ScFi and IH) and downstream detector (VH). Admixture of K^+K^- pairs was simulated with FRITIOF 6.0 [3]. This simulation has been verified by experimental measurement with time-of-flight method for two momenta of pairs: 2.90 GeV/c [4] and 4.80 GeV/c [5]. These measurements allow to normalize simulated lab momentum distribution of K^+K^- pairs. Ratio of this distribution to lab momentum distribution of $\pi^+\pi^-$ pairs is presented in Fig 1a. Distribution of $\pi^+\pi^-$ pairs is shown for comparison in Fig 1b.

Analysis with admixture K^+K^- and $p\overline{p}$ is taken as basic. Difference of breakup probabilities, obtained with and without admixture of non-pion pairs in simulated distribution of "Coulomb" pair, has been multiplied by relative error of admixture fraction measurements. From [3], [4], [5] this coefficient is estimated to be 0.25.

2 Finite size of particle production region

For analysis, Coulomb correlation function has been described by equation for point-like source:

$$A_C(Q) = \frac{2\pi m_\pi \alpha/Q}{1 - exp(-2\pi m_\pi \alpha/Q)}\,, \tag{1}$$

where m_π is a mass of charged π-meson, Q is a relative momentum in center of pair mass system, α is a fine structure constant. Work [1] describes influence of effects of finite size of particle production region, and strong interaction in a final state of pair of charged particles. Resulting correlation function differs from Eq. 2 by multiplicative correction function $F_{FSz}(Q)$ which is presented in Fig 2 (solid line). Alternative correction function has been obtained in [6]. In Fig 2 it is shown by dashed line.

Difference of breakup probabilities calculated with modified correlation function [1, 6] and correlation function (2) defines a maximal estimation of systematic error $\sigma^{FSz}_{\mathrm{syst}}$.

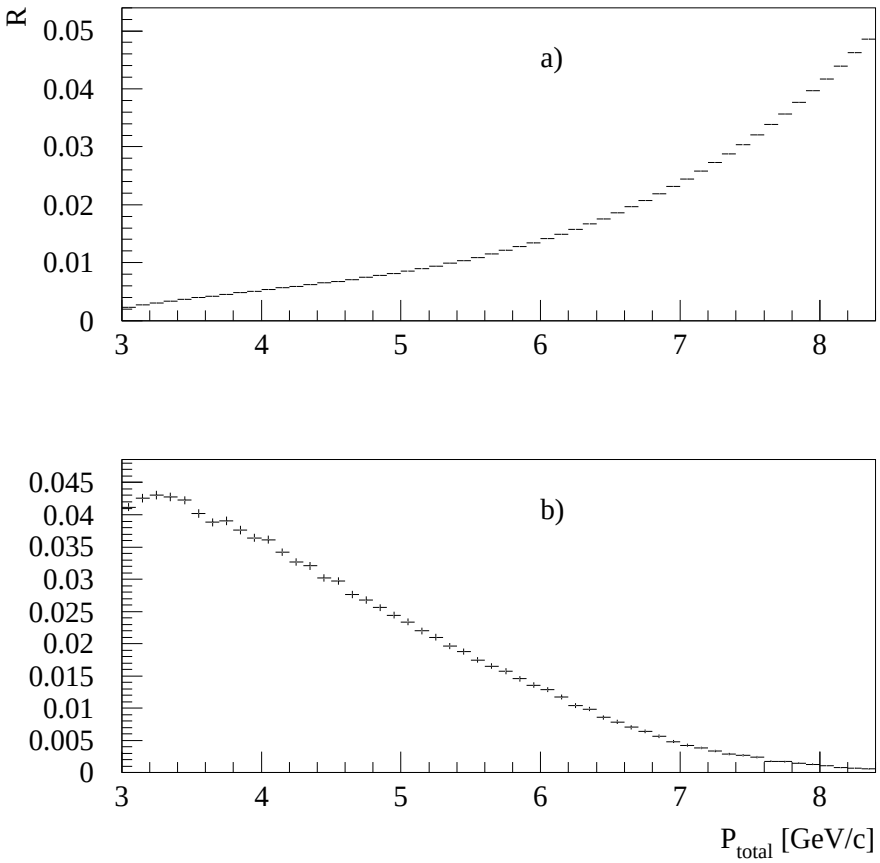

Figure 1: a) Ratio of distribution over total lab momentum of K^+K^- pairs to the same distribution of $\pi^+\pi^-$ pairs; b) distribution of $\pi^+\pi^-$ pairs over total lab momentum

3 Accuracy of multiple scattering in detectors and elements of the DIRAC setup

An average values of multiple scattering angle in detectors and aluminum membrane have been measured with an accuracy 1% [7]. Results of measurement have been introduced to GEANT-DIRAC program [8].

In contrary to investigation of other systematic errors, an error, induced by an accuracy of multiple scattering, has been estimated using additional dedicated code apart from ARIANE, GEANT-DIRAC and final fit procedure. This procedure is also partly used for systematic error occurs due to Λ correction (see section 7). This is simulation code which provide simple and fast simulation of "prompt" (sum of "atomic", "Coulomb" and "accidental under the peak of real"), "accidental", "simulated Coulomb", "simulated atomic" and "simulated non-Coulomb"

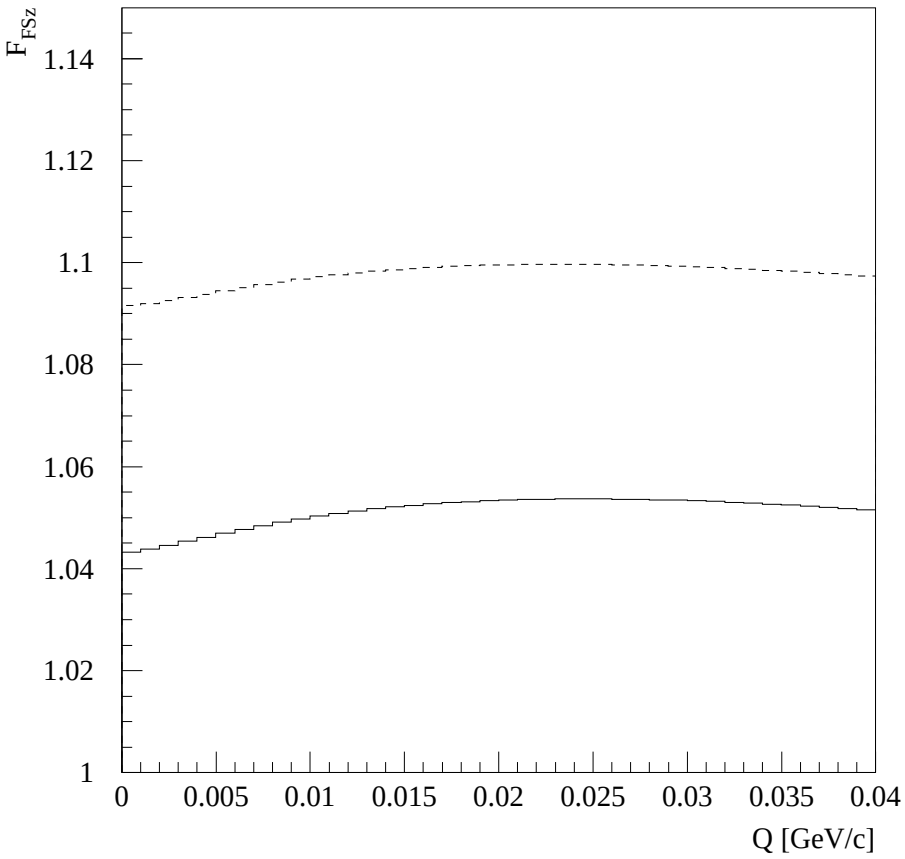

Figure 2: Correction functions for Coulomb correlation function induced by finite size of particle production region, and strong interaction in a final state

pairs. Initially events are generated uniformly over Q_X, Q_Y and Q_L.

For "Coulomb" pairs Coulomb correlation function is introduced by comparison of Coulomb weight (Eq. 2) with uniform random number in interval [0., 100.]. If weight is higher then event is accepted. At the next step initial values of Q_X, Q_Y and Q_L are varied with multiple scattering in the target (Moliere algorithm) and resolution of DIRAC setup for Q-projections:

$$Q_i = Q_i^0 + \epsilon_{Q_i}^{tag} + \sigma_{Q_i}(P_{total}) * n(0.,1.), \tag{2}$$

here Q_i^0 is initial value of i-th projection of Q ($i = X, Y, L$), $\epsilon_{Q_i}^{tag}$ is variation of Q_i in matter of target, $\sigma_{Q_i}(P_{total})$ is a resolution of the setup for Q_i-projection as function of total lab momentum of $\pi^+\pi^-$ pair, n(0.,1.) is a random value distributed according normal distribution. Values of $\sigma_{Q_i}(P_{total})$ have been estimated by ARIANE global track fit procedure, taking into account resolution of detectors and multiple scattering in the detectors, membranes (not in the

target) and air. In Fig. 3 dependencies of σ_{Q_i} on total pair momentum are presented.

Simulated "experimental" distribution is fitted by a mixture of "simulated" "atomic", "Coulomb" and "non-Coulomb" pairs with fit procedure which uses for analysis of true experimental data with background simulated by GEANT-DIRAC.

If the same sample of resolution and target description is used both for simulation of "experimental" and "simulated" data then analysis corresponds to situation when background described ideally. If resolution (or multiple scattering in the target) for "simulated" events differ from parameters used for simulation of "experimental" then systematic shift of breakup probability occurs. Comparison of two values allows to obtain an estimation of systematic error.

For investigation of influence of multiple scattering angle, σ_{Q_i} have been calculated with measured values of average angle of multiple scattering and with angles multiplied by 1.05 and 1.10 for different scatterers. Simulation of "experimental" data has been performed, using only σ_{Q_i} obtained with measured values of average multiple scattering. Simulation of "simulated" data have been used both measured and varied angles of multiple scattering. Difference of breakup probabilities allows to estimate sensitivity of result to accuracy of multiple scattering description. Table 1 presents relative change $\Delta W_{br}/W_{br}$ induced by the average angle variation for different scatterers. At simulation the breakup probability is defined to be 0.45. Multiple scattering in X- and Y-planes of ScFi varies simultaneously because of there is one measurement for both this planes [7]. Presented data show linearity of dependence of systematic breakup probability error on angle of multiple scattering for variation up to 10%.

4 Finite double-track resolution of fiber detector

If at the level of fiber detector a distance between particles of a pair is comparable with step of the fiber detector (0,43 mm) [2], the detector produce a signal only in one column with a high probability. On the other hand, only one hit in the fiber detector could be detected if the signal from the second particle is not registered due to an inefficiency of the fiber detector. In this case true distance between particles could be big (criterion on the coordinate of track at the target allows to have maximal possible distance up to 2 cm for such case). Therefore essential error occurs in measurement of a difference of coordinates of particles and an open angle of pair.

For an exception of such cases Scintillation Ionization Hodoscope (IH) is used. IH consists of 4 planes (2 in X- and 2 in Y-projections) [2]. In Fig 4 distribution of experimental events over a difference of column numbers in the X-plane of the fiber detector, associated with tracks of positively and negatively charged particles, is presented. Peak in the center and two deeps on each side are caused by difficulty of detection of close particles pairs. For pairs of the particles having only one hit in the fiber detector ("single-hit events"), the criterion on double amplitude in corresponding channels of X-planes of IH is applied. The similar criterion is used for a Y-plane of the fiber detector.

Simulated distribution of background events should to reproduce both relative height of the central peak in distribution (Fig 4), and a ratio between events which have two particles really passed through one column and given double amplitude (Fig 5b) in IH, and events which have only one particle passed through hit column and caused amplitude higher then threshold due

Table 1: Change of breakup probability due to increasing of average angle of multiple scattering in different scatterers. Analysis has been done with F ($Q_X, Q_Y < 4$ MeV/c), Q ($Q_T < 4$ MeV/c), and Q_L ($Q_T < 4$ MeV/c) and with 2-dimensional distribution Q_L, Q_T. Binning is described in Table 2

Scatterer	Average angle	$\frac{\Delta W_{br}}{W_{br}}$								
		F %	Q %	Q_L %	v1 %	v2 %	v3 %	v4 %	v5 %	v6 %
Ni	1.05	4.350	5.521	0.676	3.066	2.621	1.211	2.912	2.501	1.193
Ni	1.10	8.904	11.304	1.491	5.811	4.978	2.423	5.532	4.766	2.399
MSGC	1.05	0.805	1.067	-0.013	0.684	0.522	0.213	0.673	0.523	0.238
MSGC	1.10	1.605	2.129	-0.007	1.343	1.022	0.430	1.321	1.025	0.478
SCFIX(Y)	1.05	0.257	0.332	0.017	0.193	0.147	0.060	0.191	0.149	0.068
DeDx	1.10	0.291	0.376	0.023	0.230	0.177	0.079	0.227	0.179	0.088
Al	1.05	2.249	1.813	3.974	2.957	3.112	3.517	2.785	2.923	3.271
Al	1.10	4.442	3.588	7.873	5.795	6.103	6.940	5.450	5.722	6.443
Other	1.05	0.881	0.761	1.441	1.147	1.186	1.293	1.082	1.116	1.207
Other	1.10	1.798	1.534	2.894	2.313	2.389	2.606	2.184	2.251	2.433

to finite amplitude resolution of IH (Fig 5a).

Fig 5d shows experimental and simulated distributions over amplitude of one plane of IH for events from central peak of distribution over column number difference in the X-plane of fiber detector after applying double amplitude criterion (Fig 4). Such distribution before double amplitude cut is shown in Fig 5c. Value of a threshold for simulated events is chosen to provide the same ratio of double particle to single particle events which fit double amplitude criterion. So admixture of wrongly measured events is such as for experimental data. However, a fraction of rejected events and, as result, relative height of the central peak in distribution on a difference of fiber detector column numbers are different from experimental ones. It is caused by difficulty of adequate simulation of processes in ionization hodoscope. To provide correct description of experiment with simulated data, the weight factor for simulated events from the central peak is introduced. This version of the fiber detector response description is used as basic.

The alternative version assumes criterion on double amplitude which provides relative height of the central peak the same as at experimental distribution without taking into account a ratio of single and double particle events, satisfying to criterion. The difference of probabilities of the ionization received with an alternative and basic variants is considered as the maximum

Table 2: Versions of Q_T binning for analysis data with 2-dimensional distribution Q_L, Q_T. Criterion $Q_X < 4, Q_Y < 4$ is shown as 4'. Q_L binning is 0.5 MeV/c for all versions

Variable	Q_T binning MeV/c
v1	0-1, 1-2, 2-3, 3-4
v2	0-2, 2-3, 3-4
v3	0-3, 3-4
v4	0-1, 1-2, 2-3, 3-4, 4-4'
v5	0-2, 2-3, 3-4, 4-4'
v6	0-3, 3-4, 4-4'

estimation of systematic error $\sigma_{\rm syst}^{1-hit}$.

5 Background particles

Upstream detectors of the setup DIRAC are working at high intensity flux of particles. Therefore there is probability that pair of particles could be accompanied by one or more background particles. In some cases presence of background particles lead to misidentification of detector signals from particles of investigated pair which causes trigger signal.

The probability of such error is proportional to multiplicity of background particles. In Fig 6a an experimental distribution over multiplicity of hits in X-plane of fiber detector is shown by solid line (the minimum value is 2, because program selected events which have different hits for particle of trigger pair). Dashed line presents simulated multiplicity distribution which correspond to average intensity of a proton beam in a spill. This distribution is also shown in Fig 6b separately.

It is seen, that simulated distribution has the same average value but a shape is different. It is caused by variation of proton beam intensity during the spill. The analysis of data has shown possibility of the description of the shape and average value of distribution over multiplicity with a mixture of 61% of events simulated at half of average intensity and 39% of events at double intensity. Total distribution on multiplicity is shown in Fig 6c by solid line. For comparison an experimental distribution is shown by dashed line.

The difference of the breakup probability values obtained with multiplicity of background particles for average value of intensity and with a mixture of 2 intensities has been assumed as the maximum estimation of systematic error $\sigma_{\rm syst}^{bg}$.

6 Efficiency of the trigger

Experiment DIRAC uses the multilevel trigger which essentially reduces volume of data recorded [9]. The trigger selects events, satisfying to criteria:

$$|Q_X| < 4\text{MeV}/c\,, \tag{3}$$

$$|Q_Y| < 4\text{MeV}/c\,, \tag{4}$$

$$|Q_L| < 30\text{MeV}/c\,. \tag{5}$$

Fig 7 presents simulated efficiency of trigger as function of Q_X, Q_Y and Q_L.

It is seen that efficiency of the trigger is not uniform in the specified area. Presence of dead times and of imposed signals in the trigger electronic scheme induces essential difficulties in simulation of trigger system response. In Q-region area where efficiency varies, it can cause difference of the form experimental and simulated distributions of background events. To decrease negative effects the criterion on Q_L at final analysis has been changed to:

$$|Q_L| < 15\text{MeV}/c\,. \tag{6}$$

The deep in distribution on Q_X is occurred due to partial loss of "one-hit events". This effect is taken into account by the procedure described in section 4. Analysis of data has been performed without simulation of trigger response and with trigger response. The difference of breakup probabilities in this two cases is assumed to be the maximum estimation of the systematic error caused by non-adequate description of trigger system $\sigma^{trig}_{\text{syst}}$.

7 Correction with Λ hyperon

In [10] reconstructed width of Λ hyperon mass from experimental data is compared to simulated one. It is shown that experimental peak is wider. This difference could be corrected with introducing addition error $\sigma^{Add}_{P_{Lab}}$ in lab momentum measurement for simulated data:

$$\sigma^{Add}_{P_{Lab}} = 0.0011 P_{Lab}\,, \tag{7}$$

here P_{Lab} is lab momentum of simulated particle.

Additional error leads to change of simulated distributions of "Coulomb" and "atomic" pairs. As result breakup probability changes by some value ΔW^{Λ}_{br}. These corrections are listed in Table 3.

Analysis of reasons which induce discrepancy of Λ peak in experimental and simulated data has been done. It is found that GEANT-DIRAC program does not take into account carbon covering of cathode in drift chambers and wires in inclined drift planes (2 planes per arm). Analysis with procedure described in section 3 has shown that this reason explains 19% of effect. The reason of remained error is not known now. There is hypothesis that it is description of magnetic field [10]. But it is not proved yet. Therefore it is reasonable to think that experimentally found but non-explained correction induces systematic error which could be calculated as:

Table 3: Correction of breakup probability with Λ for analysis with different variables. For 2-dimensional analysis with Q_L, Q_T binning is described in Table 2

Variable	Q_T binning MeV/c	ΔW_{br}^{Λ}
F	$Q_X < 4, Q_Y < 4$	0.0234
Q	$Q_T < 4$	0.0189
Q_L	$Q_T < 4$	0.0415
Q_L	$Q_T < 3$	0.0429
Q_L, Q_T	v1	0.0303
Q_L, Q_T	v2	0.0319
Q_L, Q_T	v3	0.0365
Q_L, Q_T	v4	0.0286
Q_L, Q_T	v5	0.0300
Q_L, Q_T	v6	0.0338

$$\sigma_{syst}^{\Lambda} = \frac{1 - 0.19}{\sqrt{12}} \Delta W_{br}^{\Lambda}, \tag{8}$$

here factor $(1 - 0.19) = 0.81$ describes non-explained part of correction, denominator $\sqrt{12}$ occurs due to assumption that possible value of correction is uniformly distributed in a range $[0.5, 1.5]$ of calculated value.

8 Results of analysis

Tables 4,5 present estimation of systematic errors for analysis with different variables. Errors induced by an admixture of non-identified K^+K^- and $p\overline{p}$ pairs and by a correction with Λ hyperon are calculated as it is described in sections 1 and 7. For errors induced by finite double-track resolution of fiber detector, by background particles and by efficiency of the trigger, estimations of maximal errors are divided by $\sqrt{12}$ in the same assumption as in section 7. Error from finite size of particle production region is assumed to be equal to maximal value because it is pure theoretical is not used as correction.

Error induced by multiple scattering is calculated in assumptions that errors for different scatterers are independent and errors of average angle of multiple scattering for all scatterers, excluding aluminum membrane and "Other" (mainly air and mylar), equals to be 1% [7]. Error for aluminum membrane is 1.8% which is combination of accuracy of multiple scattering measurement for aluminum alloy and accuracy of thickness measurement. Error for "Other" is assumed to be 2%.

Table 4: Systematic errors of breakup probability obtained with analysis for 1-dimensional distribution

	F $Q_{X,Y} < 4$ %	Q $Q_T < 4$ %	Q_L $Q_T < 4$ %	Q_L $Q_T < 3$ %
Multiple scattering	0.56	0.60	0.70	0.73
Heavy particles admixture	0.17	0.17	0.79	0.55
Finite size effects	$^{+0.00}_{-0.62}$	$^{+0.00}_{-0.60}$	$^{+0.00}_{-0.43}$	$^{+0.00}_{-0.39}$
Double track resolution	0.33	0.41	0.03	0.05
Background particles	0.12	0.07	0.14	0.01
Trigger simulation	0.10	0.11	0.07	0.08
Correction	0.64	0.49	1.27	1.34
All systematic	$^{+0.9}_{-1.1}$	$^{+0.9}_{-1.1}$	$^{+1.7}_{-1.7}$	$^{+1.6}_{-1.7}$

References

[1] R. Lednicky, DIRAC note **2004-06** (nucl-th/0501065).

[2] B. Adeva, *et al.*, Nucl. Instr. Meth. A515 (2003) 467.

[3] O.E. Gortchakov, V.V. Yazkov, DIRAC note **2005-01** (http://dirac.web.cern.ch/DIRAC/i_notes.html)

[4] B. Adeva, *et al.*, DIRAC note **2006-05** (http://dirac.web.cern.ch/DIRAC/i_notes.html)

[5] B. Adeva, *et al.*, DIRAC note **2007-02** (http://dirac.web.cern.ch/DIRAC/i_notes.html)

[6] PHD Thesis of J. Smolik

[7] A. Dudarev, *et al.*, DIRAC note **2005-02** (http://dirac.web.cern.ch/DIRAC/i_notes.html)

[8] O. Gortchakov, DIRAC note **2007-04** (http://dirac.web.cern.ch/DIRAC/i_notes.html)

[9] L. Afanasyev *et al.*, Nucl. Instr. Meth. A491 (2002) 376. [hep-ex/0202045]

[10] O. Gortchakov, DIRAC note **2007-17** (http://dirac.web.cern.ch/DIRAC/i_notes.html)

Table 5: Systematic errors of breakup probability obtained with analysis for 2-dimensional distribution (see Table 2)

Error	v1 %	v2 %	v3 %	v4 %	v5 %	v6 %
Multiple scattering	0.59	0.60	0.63	0.56	0.56	0.58
Heavy particles admix.	0.00	0.04	0.29	0.05	0.01	0.21
Finite size effects	$^{+0.00}_{-0.55}$	$^{+0.00}_{-0.56}$	$^{+0.00}_{-0.55}$	$^{+0.00}_{-0.59}$	$^{+0.00}_{-0.60}$	$^{+0.00}_{-0.62}$
Double track resolution	0.27	0.15	0.05	0.27	0.15	0.05
Background particles	0.11	0.07	0.02	0.12	0.08	0.04
Trigger simulation	0.12	0.12	0.06	0.13	0.13	0.07
Correction	0.78	0.84	1.08	0.75	0.81	1.01
All systematic	$^{+1.0}_{-1.2}$	$^{+1.1}_{-1.2}$	$^{+1.3}_{-1.4}$	$^{+1.0}_{-1.2}$	$^{+1.0}_{-1.2}$	$^{+1.2}_{-1.3}$

A Report on 17 November 2006

On 17 November 2006 report "Systematic errors for analysis with DC and SFD and with DC only" was presented at the DIRAC Collaboration meeting. Slides for this report are presented in this appendix. Figures from slides are started from number 8.

Some results are obsolete now. For example systematic error, induced by multiple scattering, was calculated in assumption that error of measurement is correlated for all scatterers. Error in aluminum membrane was underestimated (1% instead of 1.8%). Different correlation function was used for finite size effects. There was not estimation of error due to Λ correction.

But this report proved using 3-parametric fit with simulated "atomic", "Coulomb" and "non-Coulomb" pairs. Because this method provides better statistical accuracy and compatible systematic errors relatively to "2-parametric" fit which uses mixture of simulated "Coulomb" and "non-Coulomb" pairs in region where "atomic" pairs absent, following with extrapolation of background description to the region of "atomic" pairs.

Also there was comparison of errors for versions of analysis with DC and ScFi and with DC only.

Fraction of single particle events among 1-hit SFD events and fraction of double track events which fit criterion on double amplitude in IH planes.

Plane	Data	Single %	Accepted double %
1	Exp	11.03	88.82
1	MC	11.02	98.14
2	Exp	12.22	89.89
2	MC	12.31	98.59
3	Exp	9.36	89.24
3	MC	9.30	98.19
4	Exp	9.82	88.85
4	MC	9.81	97.53

Weight coefficients for simulated 1-hit SFD events.

Projection	From amplitude analysis	Additional
X	0.830	0.8468
Y	0.831	0.9259

Simulated values of relative statistical and sistematic errors of break up probability for Ni2001 (94 μm). F ($Q_X < 4, Q_Y < 4$ MeV/c)

Cut	$\sigma_{\rm stat}$ %	$\sigma_{\rm syst}^{MS1\%}$ %	$\sigma_{\rm syst}^{K+K-}$ %	$\sigma_{\rm syst}^{FSz}$ %	$\sigma_{\rm syst}^{1-hit}$ %	$\sigma_{\rm syst}^{bg}$ %	$\sigma_{\rm syst}^{trig}$ %
Accidental background							
0.5	27.958						
1.0	12.698						
1.5	8.377						
2.0	7.686						
2.5	8.125						
3.0	9.283						
3.5	10.620						
4.0	12.318						
Simulated background							
0.5	12.07	3.414	-0.08	-1.17	-2.64	5.04	1.32
1.0	6.24	3.300	0.63	-1.15	-3.11	3.57	0.85
1.5	5.21	2.650	0.68	-1.28	-2.55	0.86	0.73
2.0	5.51	2.190	0.54	-1.41	-2.05	0.91	0.70
2.5	6.33	1.862	0.27	-1.55	-2.06	1.34	0.70
3.0	7.54	1.568	-0.17	-1.79	-1.97	1.34	0.67
3.5	8.94	1.334	-0.80	-2.08	-1.95	2.56	0.45
4.0	10.43	1.170	-1.81	-2.50	-1.89	2.71	0.57
Fit with "atomic pair" signal							
23.	4.61	2.536	1.25	-1.02	-2.52	0.96	0.78

Simulated values of relative statistical and sistematic errors of break up probability for Ni2001 (94 μm). Q ($Q_X < 4, Q_Y < 4$ MeV/c)

Cut	$\sigma_{\rm stat}$ %	$\sigma^{MS1\%}_{\rm syst}$ %	$\sigma^{K+K-}_{\rm syst}$ %	$\sigma^{FSz}_{\rm syst}$ %	$\sigma^{1-hit}_{\rm syst}$ %	$\sigma^{bg}_{\rm syst}$ %	$\sigma^{trig}_{\rm syst}$ %
Accidental background							
0.5	22.866						
1.0	10.673						
1.5	8.142						
2.0	8.282						
2.5	9.267						
3.0	10.792						
3.5	12.633						
Simulated background							
0.5	10.80	3.348	0.57	-1.20	-2.43	4.16	0.85
1.0	5.97	3.092	1.07	-1.28	-3.87	1.98	0.86
1.5	5.58	2.524	1.19	-1.45	-2.83	0.13	0.68
2.0	6.29	2.196	1.18	-1.65	-2.69	0.08	1.00
2.5	7.49	1.910	0.98	-2.01	-2.79	-0.89	0.68
3.0	9.10	1.678	0.63	-2.40	-2.54	-0.19	0.28
3.5	10.91	1.504	0.17	-2.95	-2.51	0.43	0.52
Fit with "atomic pair" signal							
15.	4.94	2.718	1.43	-1.06	-3.18	0.51	0.89

Simulated values of relative statistical and sistematic errors of break up probability for Ni2001 (94 μm). Q ($Q_T < 4$ MeV/c)

Cut	$\sigma_{\rm stat}$ %	$\sigma^{MS1\%}_{\rm syst}$ %	$\sigma^{K+K-}_{\rm syst}$ %	$\sigma^{FSz}_{\rm syst}$ %	$\sigma^{1-hit}_{\rm syst}$ %	$\sigma^{bg}_{\rm syst}$ %	$\sigma^{trig}_{\rm syst}$ %
Accidental background							
0.5	23.528						
1.0	11.395						
1.5	9.172						
2.0	9.775						
2.5	11.308						
3.0	13.475						
3.5	16.039						
4.0	19.064						
Simulated background							
0.5	11.34	3.346	-0.23	-1.19	-2.26	4.27	1.09
1.0	6.83	3.066	0.13	-1.27	-3.66	2.06	1.11
1.5	6.86	2.476	0.03	-1.44	-2.61	0.25	1.01
2.0	8.07	2.116	-0.28	-1.63	-2.40	0.25	1.39
2.5	9.86	1.786	-0.91	-1.96	-2.38	-0.58	1.19
3.0	12.18	1.508	-1.65	-2.32	-2.05	0.15	0.94
3.5	14.79	1.278	-2.64	-2.81	-1.88	0.61	1.30
4.0	17.53	1.094	-3.55	-3.03	-1.75	0.81	1.92
Fit with "atomic pair" signal							
15.	5.09	2.774	1.33	-0.84	-3.13	0.56	0.83

Simulated values of relative statistical and sistematic errors of break up probability for Ni2001 (94 μm). Q_L ($Q_T < 4$ MeV/c)

Cut	$\sigma_{\rm stat}$ %	$\sigma^{MS1\%}_{\rm syst}$ %	$\sigma^{K+K-}_{\rm syst}$ %	$\sigma^{FSz}_{\rm syst}$ %	$\sigma^{1-hit}_{\rm syst}$ %	$\sigma^{bg}_{\rm syst}$ %	$\sigma^{trig}_{\rm syst}$ %
Accidental background							
0.5	10.386						
1.0	10.612						
1.5	12.132						
2.0	14.036						
Simulated background							
0.5	8.00	1.196	-5.07	-1.90	-0.86	1.43	0.61
1.0	9.11	0.920	-4.84	-2.18	-0.66	2.53	0.63
1.5	10.90	0.730	-5.03	-2.47	-1.07	2.61	0.64
2.0	12.56	0.692	-5.44	-2.81	-1.40	3.33	0.71
Fit with "atomic pair" signal							
15.	7.05	1.176	-4.59	-1.49	-0.25	1.10	0.55

Simulated values of relative statistical and sistematic errors of break up probability for Ni2001 (94 μm). Q_L ($Q_T < 3$ MeV/c)

Cut	$\sigma_{\rm stat}$ %	$\sigma_{\rm syst}^{MS1\%}$ %	$\sigma_{\rm syst}^{K+K-}$ %	$\sigma_{\rm syst}^{FSz}$ %	$\sigma_{\rm syst}^{1-hit}$ %	$\sigma_{\rm syst}^{bg}$ %	$\sigma_{\rm syst}^{trig}$ %
Accidental background							
0.5	9.879						
1.0	10.119						
1.5	11.383						
2.0	13.009						
Simulated background							
0.5	7.76	1.482	-3.61	-1.91	-1.05	0.22	0.47
1.0	8.84	1.256	-3.29	-2.10	-1.01	1.05	0.51
1.5	10.41	1.072	-3.42	-2.34	-1.45	1.11	0.36
2.0	11.81	1.046	-3.65	-2.56	-1.69	1.61	0.36
Fit with "atomic pair" signal							
15.	6.75	1.508	-3.26	-1.53	-0.40	-0.08	0.58

Simulated values of relative statistical and sistematic errors of break up probability for Ni2001 (94 μm). Analysis is done with 1-dimensional distribution over F, Q and Q_L. Fit uses simulated "atomic pair" signal

Variable	$\sigma_{\rm stat}$ %	$\sigma^{MS1\%}_{\rm syst}$ %	$\sigma^{K+K-}_{\rm syst}$ %	$\sigma^{FSz}_{\rm syst}$ %	$\sigma^{1-hit}_{\rm syst}$ %	$\sigma^{bg}_{\rm syst}$ %	$\sigma^{trig}_{\rm syst}$ %
F $(Q_X < 4, Q_Y < 4)$	4.61	2.536	1.25	-1.02	-2.52	0.96	0.78
Q $(Q_X < 4, Q_Y < 4)$	4.94	2.718	1.43	-1.06	-3.18	0.51	0.89
Q $(Q_T < 4)$	5.09	2.774	1.33	-0.84	-3.13	0.56	0.83
Q_L $(Q_T < 4)$	7.05	1.176	-4.59	-1.49	-0.25	1.10	0.55
Q_L $(Q_T < 3)$	6.75	1.508	-3.26	-1.53	-0.40	-0.08	0.58

Simulated values of relative statistical and sistematic errors of break up probability for Ni2001 (94 μm). Analysis is done with 2-dimensional distribution over Q_L and Q_T. Fit uses simulated "atomic pair" signal

Q_T bins	$\sigma_{\rm stat}$ %	$\sigma^{MS1\%}_{\rm syst}$ %	$\sigma^{K+K-}_{\rm syst}$ %	$\sigma^{FSz}_{\rm syst}$ %	$\sigma^{1-hit}_{\rm syst}$ %	$\sigma^{bg}_{\rm syst}$ %	$\sigma^{trig}_{\rm syst}$ %
0-1, 1-2, 2-3, 3-4	4.77	2.248	0.26	-1.24	-2.08	0.87	0.92
0-2, 2-3, 3-4	4.98	2.112	0.00	-0.89	-1.16	0.57	0.93
0-3, 3-4	5.89	1.590	-1.63	-1.08	-0.36	0.14	0.44
0-1, 1-2, 2-3, 3-4, 4-4'	4.62	2.218	0.42	-1.01	-2.04	0.96	0.99
0-2, 2-3, 3-4, 4-4'	4.81	2.094	0.18	-1.04	-1.17	0.65	1.00
0-3, 3-4, 4-4'	5.65	1.604	-1.33	-1.25	-0.40	0.29	0.56

Simulated values of relative statistical and sistematic errors of break up probability for Ni2001 (94 μm) without upstream detectors.
Q ($Q_T < 6$ MeV/c)

Cut	$\sigma_{\rm stat}$ %	$\sigma_{\rm syst}^{MS1\%}$ %	$\sigma_{\rm syst}^{K+K-}$ %	$\sigma_{\rm syst}^{FSz}$ %	$\sigma_{\rm syst}^{trig}$ %
Accidental background					
0.5	64.441				
1.0	24.669				
1.5	17.004				
2.0	14.167				
2.5	13.070				
3.0	12.828				
3.5	13.022				
4.0	13.456				
Simulated background					
0.5	37.28	5.038	-7.26	2.99	8.63
1.0	15.93	3.812	-6.98	3.67	7.00
1.5	11.43	4.094	-10.07	6.20	10.97
2.0	9.82	4.072	-13.95	9.41	13.53
2.5	9.37	4.084	-18.88	12.81	18.80
3.0	9.38	4.079	-39.46	26.92	39.64
3.5	9.63	3.944	-70.44	50.32	68.59
4.0	10.19	3.702	-78.66	62.28	73.14
Fit with "atomic pair" signal					
15.	10.24	5.110	-21.41	15.94	20.15

Simulated values of relative statistical and sistematic errors of break up probability for Ni2001 (94 μm) without upstream detectors.
Q_L ($Q_T < 8$ MeV/c)

Cut	$\sigma_{\rm stat}$ %	$\sigma_{\rm syst}^{MS1\%}$ %	$\sigma_{\rm syst}^{K+K-}$ %	$\sigma_{\rm syst}^{FSz}$ %	$\sigma_{\rm syst}^{trig}$ %
Accidental background					
0.5	10.959				
1.0	10.824				
1.5	12.365				
2.0	14.374				
Simulated background					
0.5	8.17	1.336	-12.39	0.61	4.76
1.0	8.67	1.153	-13.38	1.32	5.45
1.5	10.36	0.942	-13.02	2.06	5.69
2.0	12.12	0.880	-13.93	3.12	6.21
Fit with "atomic pair" signal					
15.	7.32	1.343	-12.31	-0.14	4.48

Simulated values of relative statistical and sistematic errors of break up probability for Ni2001 (94 μm) without upstream detectors.
Q_L ($Q_T < 6$ MeV/c)

Cut	$\sigma_{\rm stat}$ %	$\sigma_{\rm syst}^{MS1\%}$ %	$\sigma_{\rm syst}^{K+K-}$ %	$\sigma_{\rm syst}^{FSz}$ %	$\sigma_{\rm syst}^{trig}$ %
Accidental background					
0.5	10.381				
1.0	10.288				
1.5	11.787				
2.0	13.636				
Simulated background					
0.5	7.83	1.873	-8.29	-1.06	3.54
1.0	8.41	1.728	-8.45	-1.24	4.02
1.5	10.03	1.623	-8.16	-1.39	4.26
2.0	11.69	1.610	-8.51	-1.64	4.61
Fit with "atomic pair" signal					
15.	6.97	1.896	-8.25	-0.85	3.26

Simulated values of relative statistical and sistematic errors of break up probability for Ni2001 (94 μm) without upstream detectors. Analysis is done with 2-dimensional distribution over Q_L and Q_T. Fit uses simulated "atomic pair" signal

Q_T bins	$\sigma_{\rm stat}$ %	$\sigma_{\rm syst}^{MS1\%}$ %	$\sigma_{\rm syst}^{K+K-}$ %	$\sigma_{\rm syst}^{FSz}$ %	$\sigma_{\rm syst}^{trig}$ %
0-2, 2-4, 4-6, 6-8	6.11	2.679	-6.46	-3.68	4.67
0-4, 4-6, 6-8	6.17	2.584	-6.54	-3.75	4.52
0-6, 6-8	6.57	1.940	-8.02	-3.34	4.36

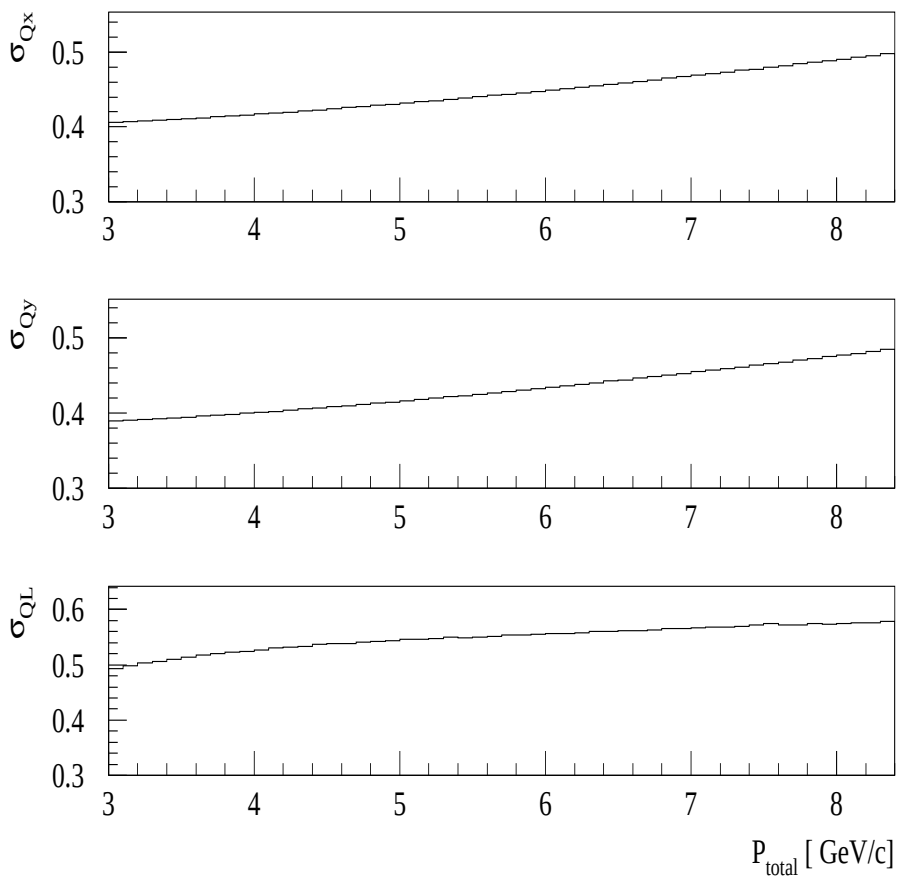

Figure 3: Dependence of resolution of DIRAC setup for projections of Q on total pair momentum. σ_{Q_X}, σ_{Q_Y}, and σ_{Q_L} are presented in MeV/c, but P_{total} is in GeV/c

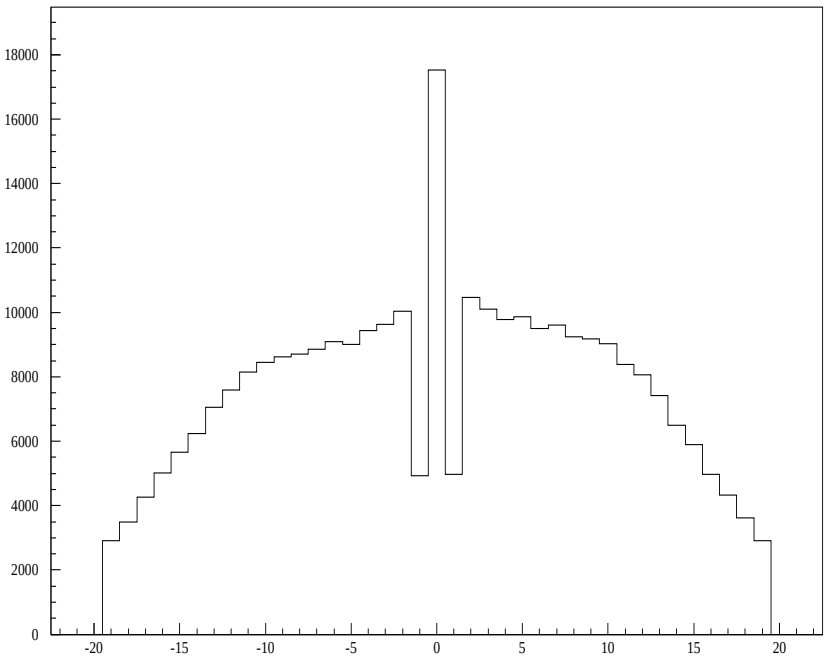

Figure 4: Experimental distribution of prompt $\pi^+\pi^-$ pairs over a difference of numbers of hit columns in the X-plane of the fiber detector

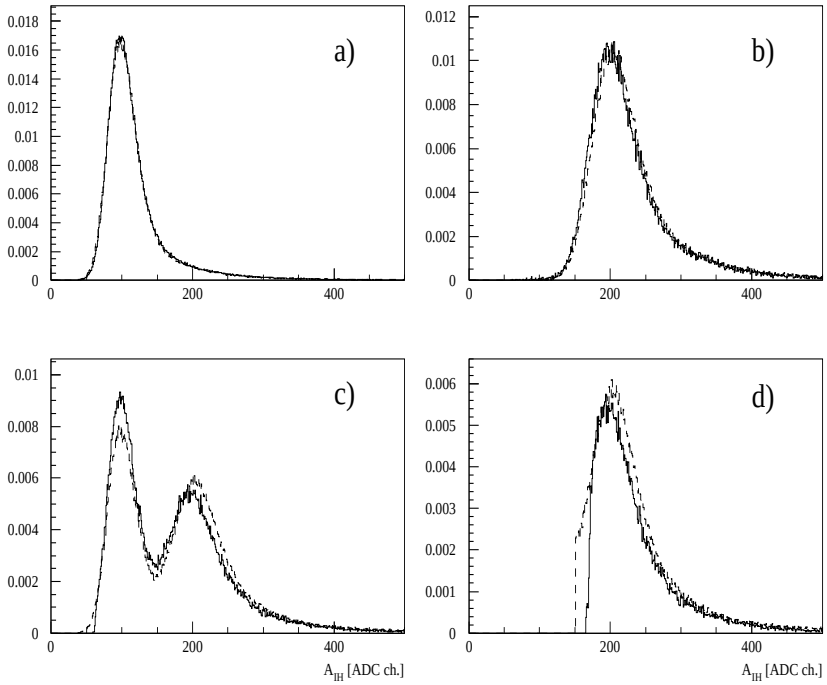

Figure 5: Distributions over amplitude of one plane of ionization hodoscope (IH) for experimental (solid line) and simulated (dashed line) events: (a) single particle events; (b) double particle events; (c) events from central peak of distribution over column number difference in the X-plane of fiber detector; (d) distribution (c) after applying of double-amplitude criterion

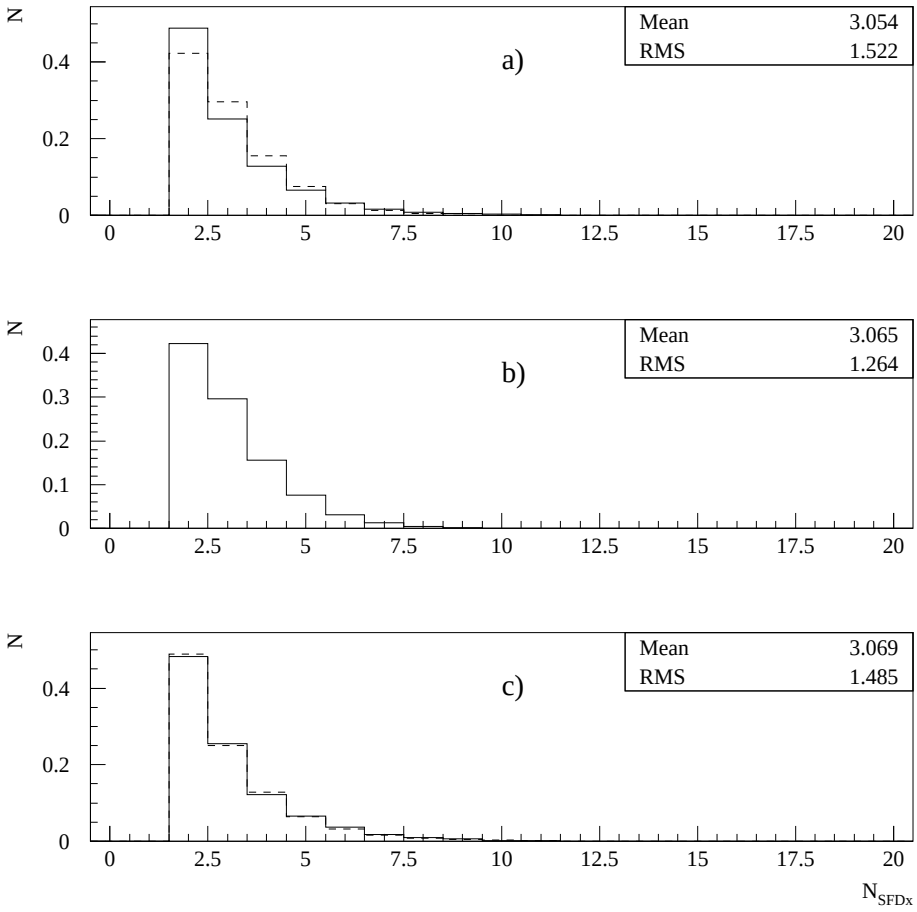

Figure 6: Distributions over multiplicity of hits in X-plane of fiber detector

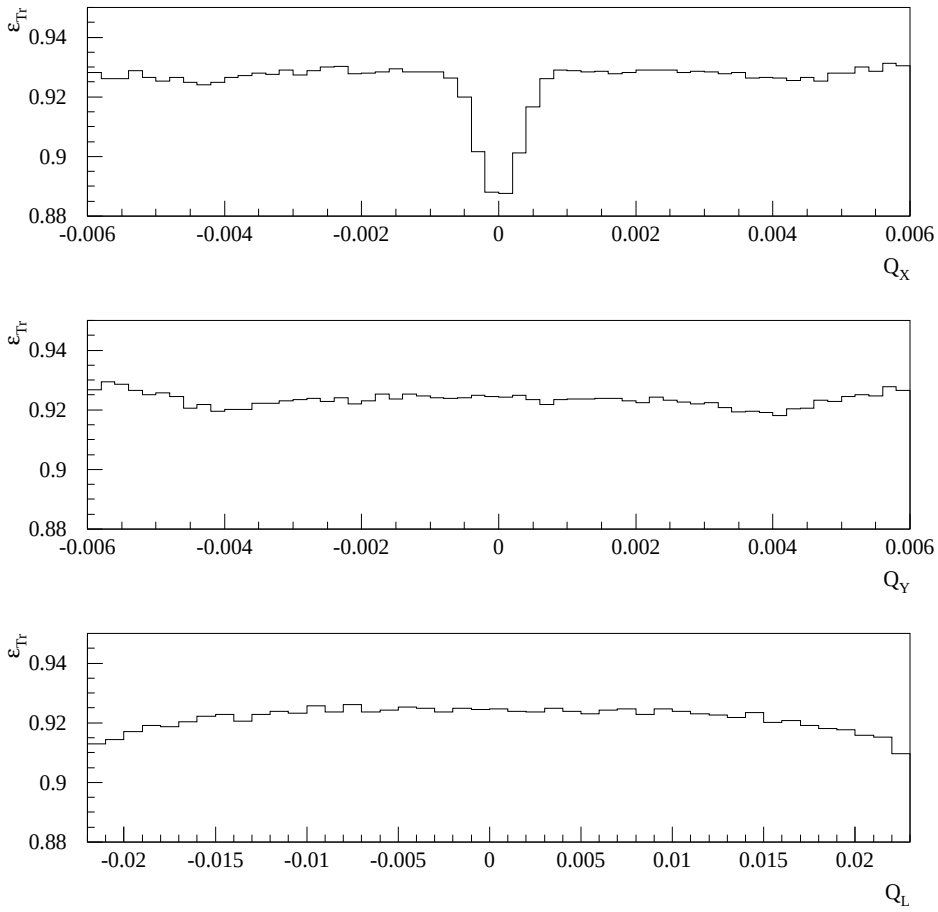

Figure 7: Efficiency of trigger as function of relative momentum Q projections: Q_X, Q_Y and Q_L

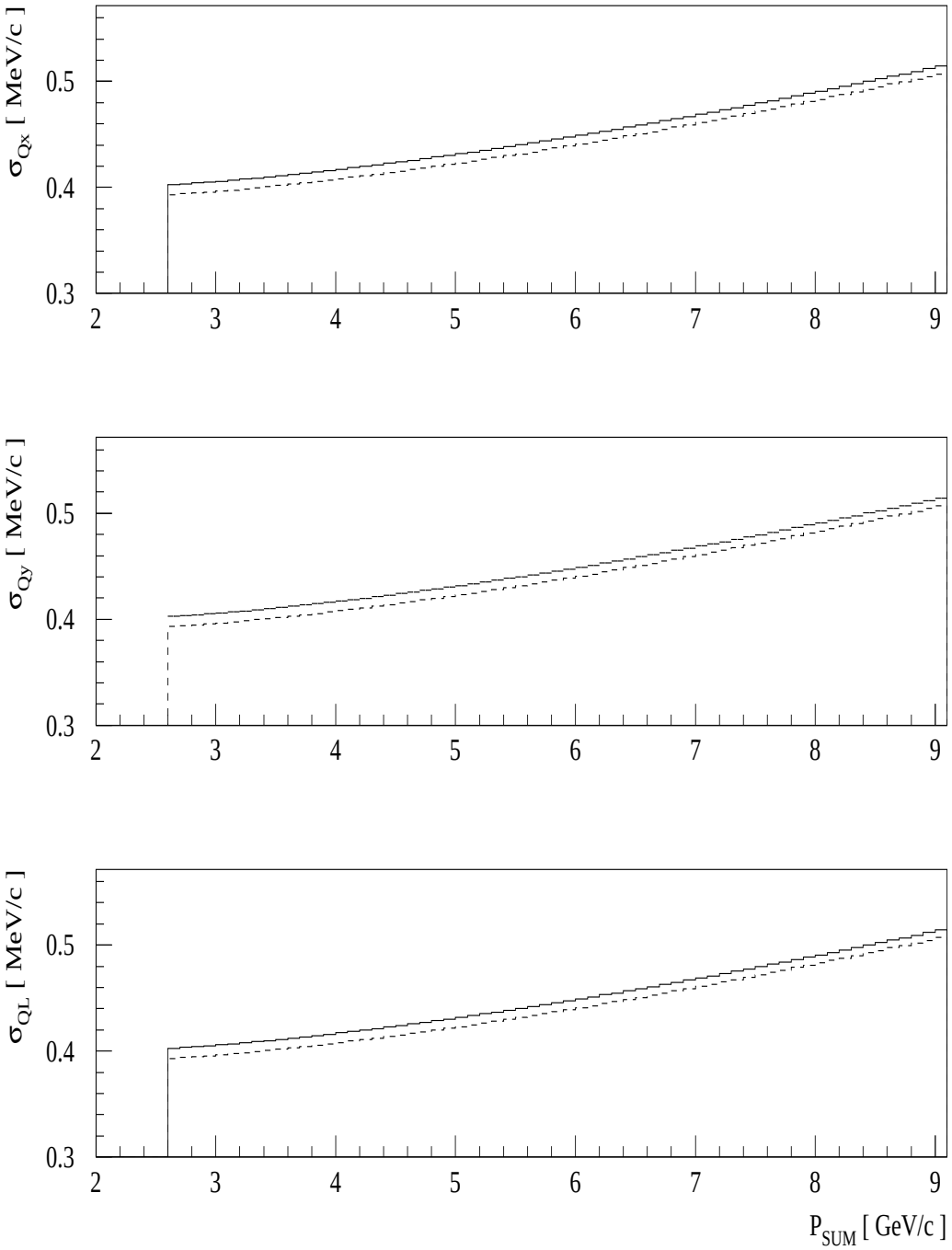

Figure 8: Resolution with expected multiple scattering (solid) and decreased by 5%

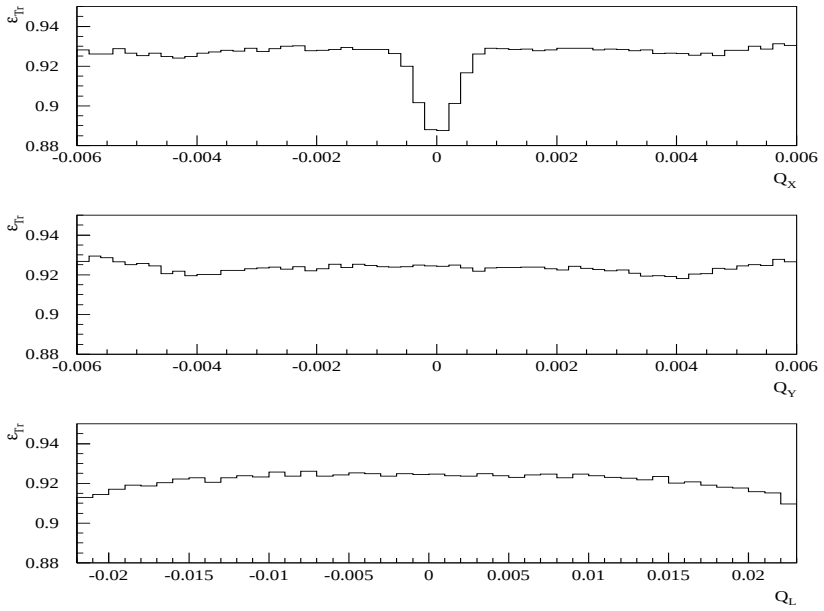

Figure 9: Efficiency of T4 (solid) and (DNA+RNA)*T4

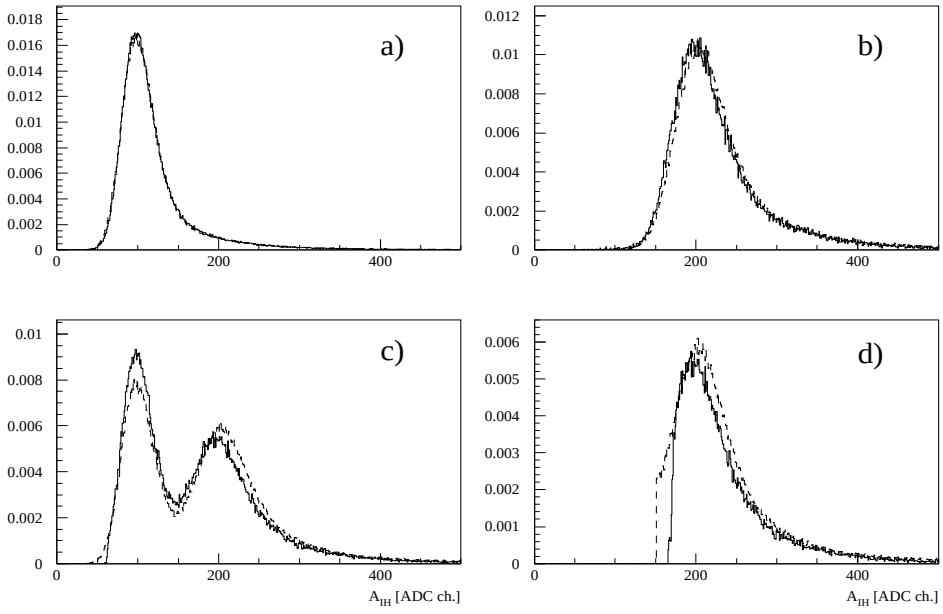

Figure 10: IH amplitudes: experimental (solid) and simulated (dashed)